Aerodynamics of Large Rotors
WP2
Deliverable 2.4

Authors: Martin O.L.Hansen[1],Niels N. Sørensen[1], N.Ramos-García[1], Liesbeth Florentie[2], Koen Boorsma[6], Ozlem Ceyhan[6], Gaël de Oliveira[2], Daniel Baldacchino[2], Sugoi Gomez Iradi[3], Beatriz Méndez López[3], Arturo Muñoz[3], J. Prospathopoulos[4], G. Papadakis[4], S. Voutsinas[4], G.Barakos[5],Y. Wang[5], V. Leble[5].

[1] Technical University of Denmark, [2] Delft University of Technology, [3] National Renewable Energy Centre (CENER), [4] National Technical University of Athens, [5] University of Liverpool. [6] ECN

Date: Sept 2015

Agreement n.: FP7-ENERGY-2013-1/ n° 608396

Duration: November 2013 to November 2017

Coordinator: ECN Wind Energy, Petten, The Netherlands

Supported by

This project has received funding from the European Unionś Seventh Programme for research, technological development and demonstration under grant agreement No FP7-ENERGY-2013-1/ n ° 608396

1 Introduction

This report is written on the basis of Delivery D2.1, Supplement to Delivery D2.1 and Delivery 2.3 from WP2 in the AVATAR project, [2], [3] and [4]. Delivery 2.1 concerns use of 2-D CFD codes ranging from viscous-inviscid interaction codes and full compressible and incompressible Navier-Stokes solvers. Delivery WP2.3 concerns full Power Curve Predictions.

2 Discussion of 2-D aerodynamics results and recommendations

The 2-D airfoil computations were performed using following codes

Q3UIC - A panel method including integral boundary layer equations

RFOIL - Panel code - similar to XFOIL but with improvements

MaPFlow - a compressible N-S code

WMB - a compressible N-S code

HMB2 - a slightly different vesion of WMB

EllipSys - an incompressible N-S code

OpenFoam - an incompressible open source N-S code

CRES - in house code

More details on the various codes can be found in D2.1 and the supplementary to D2.1. It should also be mentioned that all the N-S solvers used the k- ω turbulence model.

The results shown in Delivery 2.1 are only the integrated lift and drag as function of angle of attack, whereas the supplementary report contains distributed pressure and skinfriction along the airfoil and reveals some of the differences seen in the overall lift and drag.

A general conclusion is that the spread in the results were higher than expected, and increasing with the airfoil thickness. However, it is known that thick airfoils are difficult to compute, since the boundary layer may become close to separation even at low angles of attack and that the flow is expected to be more 3-D than for the thinner ones. Further, the transition is more difficult to compute due to a generally less distinct pressure gradient.

In the following results are shown for the 24 % thick DU 91-MOD240, since extra computations were performed for this one. Figures 1 and 2 show the computed lift coefficient as function of the angle of attack from most of the full N-S used in AVATAR for Re=20×10^6 and for fully turbulent flow. It is seen that the codes agree quite well on the lift in the linear region with some differences in stall. There is no clear trend

whether the compressible codes (MapFlow, WMB and HMB2) give a different result than the incompressible codes (EllipSys and OpenFoam). Figures 3 and 4 show the computed drag coefficient using the same codes for fully turbulent flow and Re=20×10^6. Especially Figure 4 for the lower angles of attack show a big difference between the codes, where the WMB code grossly underestimates the minimum drag coefficient compared to most of the other codes, and also HMB2 is rougly 10 drag counts lower that the other codes. It is seen that the two incompressible codes (EllipSys and OpenFoam) give very similar results around the minimum drag.

Figure 5 shows the pressure coefficient over the airfoil at an angle of attack of 8 degrees, Re=20×10^6 and fully turbulent flow. It is seen that the codes predict very similar pressure distributions below stall, which also give the same lift as seen in Figures 1 and 2. However, when plotting the skin friction one can see the cause of the differences in the minimum drag coefficient, see Figure 6. It is quite significant that the skin friction precticted by some of the compressible codes are significantly lower than the incompressible codes. Also it was discovered that some of the compressible codes show a much higher grid dependency than the incompressible ones. This can be seen in Figures 7 and 8 showing respectively the computed drag as function of the angle of attack and the skinfriction at an angle of attack of 8 degrees using the HMB2 code on two different grids. With the grid OG (own grid) the results become much closer to most of the other CFD codes. So the question is if the compressible codes are more sensitive to the resolution of the innermost boundary layer, where the local Mach numbers are small or that difference is a compressible effect. At least the two incompressible codes agree very well on their result and they also agree quite well with XFOIL, at least before stall, so it is believed that the incompressible N-S equations are solved reasonably accurately. To validate the codes further, and not just comparing them against each other, it would be a good idea to find and compute a case with some high fidelty measurements of the skin friction.

In the project two other viscous-inviscid methods are also applied, where the potential flow is coupled to the integral boundary layer equations that are closedwith some empirical expressions. One is the RFOIL, which is a modified XFOIL. The results, as shown in Deliverable 2.1, are close to the results from the other codes and seem to give a slightly lower minimum drag than the EllipSys results. The problem with their code is that the integral boundary layer equation is not valid when the flow becomes massively stalled and XFOIL is known to generally overpredict Cl,max. The other viscous-inviscid code is the QUICK code from DTU Wind Energy. This code also has as a Karman-Tsien correction for moderate compressibility effects and a transition model. The drag is not computed integrating the skin friction and pressure distribution, but instead the Squire-Young equation is used. It is seen in in the supplement to Deliverable 2.1 that the skin friction distribution is quite different from the N-S based codes, but the drag computed in the turbulent cases are reasonable but when transition is included the drag seems too high.

It was previously shown that the $\gamma - \theta$ transition model from Menter becomes insensitive when the Re number becomes high [1] and can therefore not be used on the very large turbines. Instead all the partners that delivered results for the transitional case (EllipSys, WMB, QUICK and RFOIL) used the e^N method. In Figures 9 and 10 are plotted, respectively, the resulting lift versus angle of attack and drag versus angle of attack for as well the turbulent and transitional case using the EllipSys code. It is clearly seen that the known qualitative effect of higher maximum lift and lower minimum drag when transition is included, even for the high Re number of Re=20×10^6.

To sum up the observations of the 2-D results it is concluded that the spread in the results, especially around

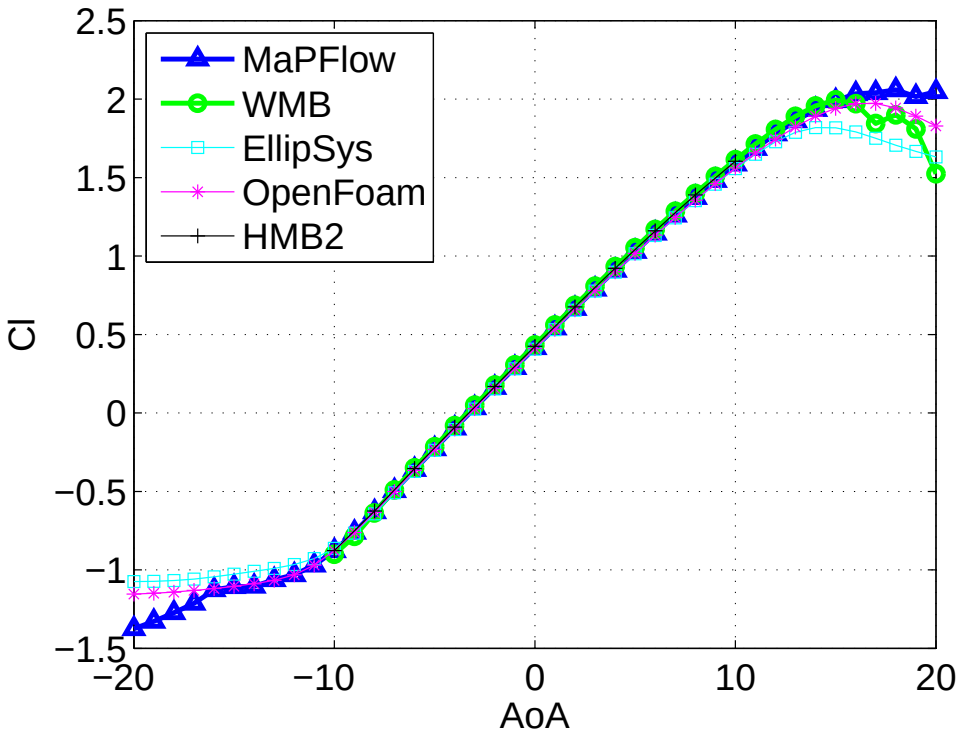

Figure 1: lift vs AoA.

the minimum the drag were higher than anticipated. It seems that the spread is caused by a difference in the skin friction and the question is then whether it is an compressible effect or if the compressible solvers are more sensitive to the grids. It could perhaps be recommended to look for some experiments that can be used to validate the capabilities of the various codes to predict the skin friction distribution. Also it is recommended to define better the sign of the skinfriction C_f, since there seems to be some inconsistencies in the results uploaded to the AVATAR homepage. The lift and drag coefficients should in the future also be divided into a pressure part and a friction part.

3 Discussion of power curve predictions and recommendations

For the 3-D rotor computations the following codes were used.

MIRAS - A 3-D panel code where the BL is coupled with QUICK that gives a chordwise transpiration velocity as function of the local angle of attack

Aero-Module - A BEM based or lifting line free vortex formulation AWSM

MaPFlow - a compressible N-S code

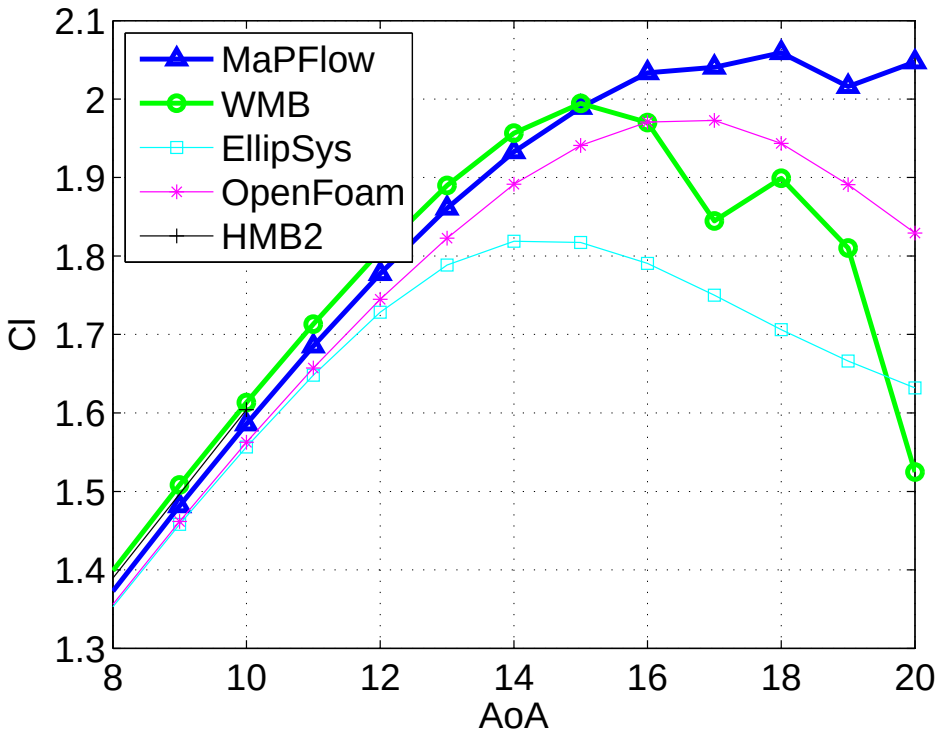

Figure 2: lift vs AoA

HMB2 - a compressible NS code

EllipSys - an incompressible N-S code

UMPM - A free wake 3D unsteady multibody panel method

FLOWer code - a compressible NS code

Only the MapFlow, HMB2, EllipSys and FLOWer code are full Navier-Stokes solvers, and from these only EllipSys has delivered transitional data that has been compared to the panel codes with a reasonable agreement in the mechanical power and thrust up to rated wind speed, except for the MIRAS code giving slightly lower thrust values than the others. However, these results are not so interesting since they strongly depend, with the exception of EllipSys and MIRAS on prescribed airfoil data. MIRAS uses the viscous-inviscid panel code QUICK to predict transpiration velocities along the airfoils for different angles of attack. The results for MIRAS and the other not Navier-Stokes solvers can be found in Deleverable D2.3

What is much more interesting is how the N-S based codes compare to each other, which was only done for the fully turbulent flows. Figures 11 and 12 show respectively the computed power and thrust for the AVATAR reference rotor assuming fully turbulent boundary layers. From Figure 12 can be seen that the

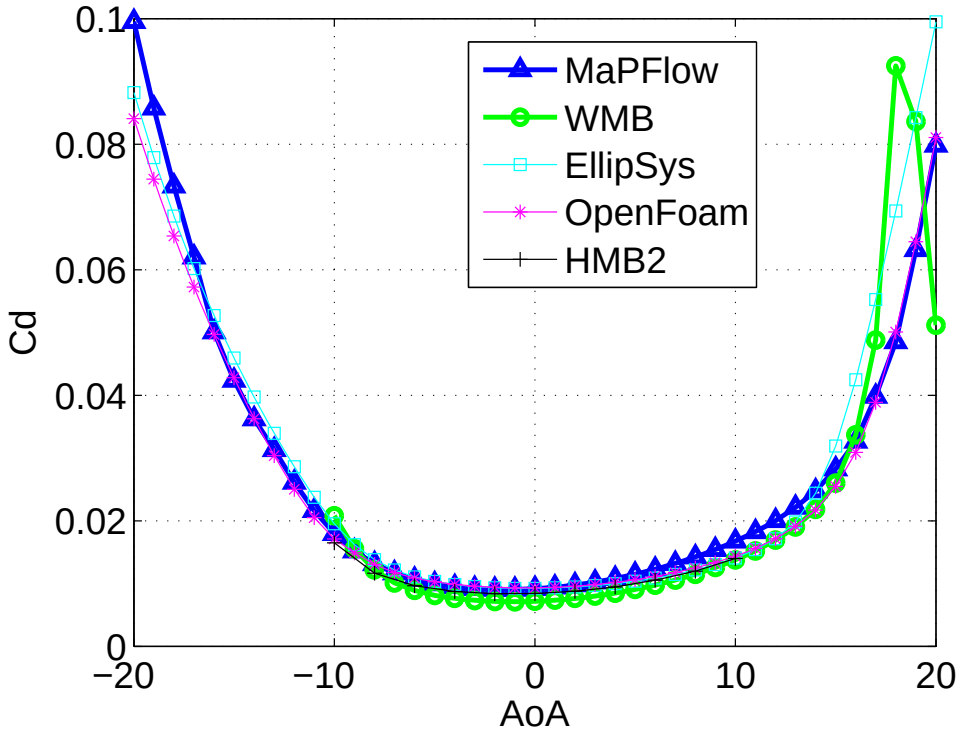

Figure 3: Drag vs. AoA

various codes more or less agree on the thrust force, which is mostly pressure dominated. But in Figure 11 it is seen that the two runs of the HMB2 code from respectively Cener and University of Liverpool predicts higher power than the three other Navier-Stokes codes, EllipSys, MapFlow and FLOWer. It should be noted that EllipSys solves the incompressible Navier-Stokes equations and MapFlow and FLOWer are compressible codes, and therefore it is believed that the difference between the HMB2 code ond the others is not a compressible effect. From Figure 13 showing the pressure distribution at r=70 m for V_o=9 m/s it is seen that all the five different CFD solvers agree very well on the pressure distribution, which is the reason that they all agree on the thrust curve. However, Figure 14 showing the skin friction at at r=70 m for V_o=9 m/s shows, just as in the 2-D case a large difference between the codes. This is also seen in the radial force distributions in Figures 15 and 16 showing respectively the tangential and normal loads for V_o=9 m/s for the Avatar reference rotor, where the normal distributions are much more similarthan the tangential ones.

4 Conclusion

It is concluded that the spread, especially around the minimum drag, were higher than anticipated for the 2-D codes. It is shown that this difference is strongly related to the skinfriction distributions and since this work only concerns code to code validation it would be preferable if additionally to compare with reliable measured data. There will in the AVATAR project also be made some integrated data for the drag at high Reynolds numbers in the high pressure wind tunnel. It is also seen that some of the compressible codes show a higher grid dependency than the incompressible codes, that could indicate some convergence problems near

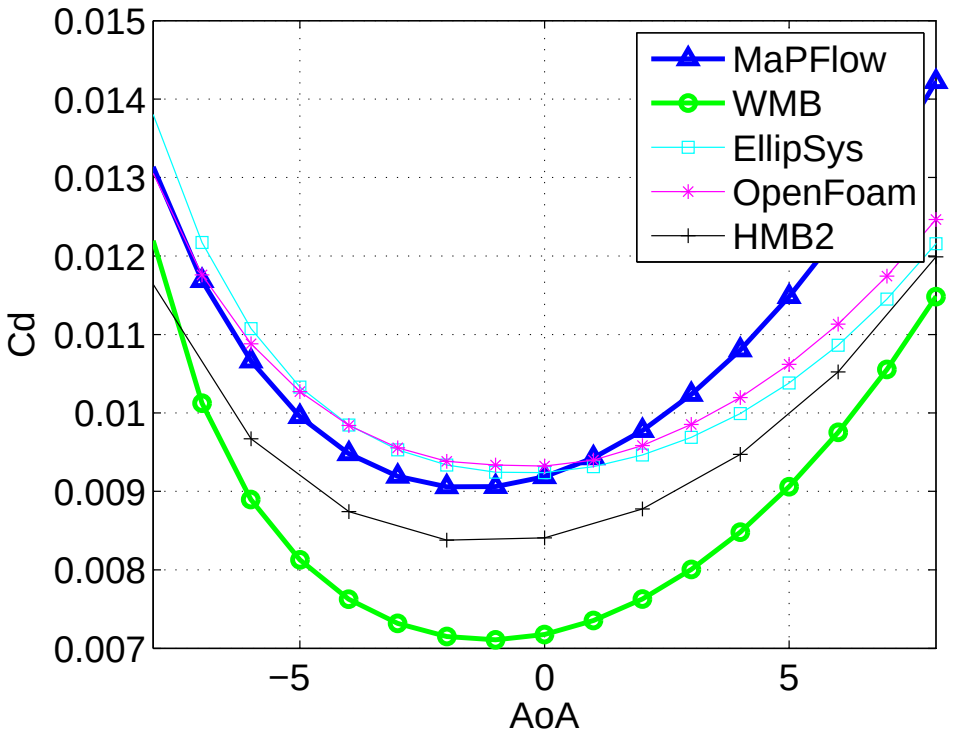

Figure 4: Drag vs AoA

the wall where the local Mach numbers are low.

For the 3-D rotor computations it is seen that transition still plays a role, even for the very large rotors where the transition is moved towards the leading edge due to the higher Reynolds numbers. Efforts should be made to include transition in future simulations. Three of the four Navier-Stokes based solvers agree quite well on both the integral values as power and thrust as function of wind speed, but also the pressure and skin friction distributions looks quite similar. Since the three codes are a mix of compressible and incompressible codes it seems that the compressible effects are not very large for the 20 MW AVATAR rotor.

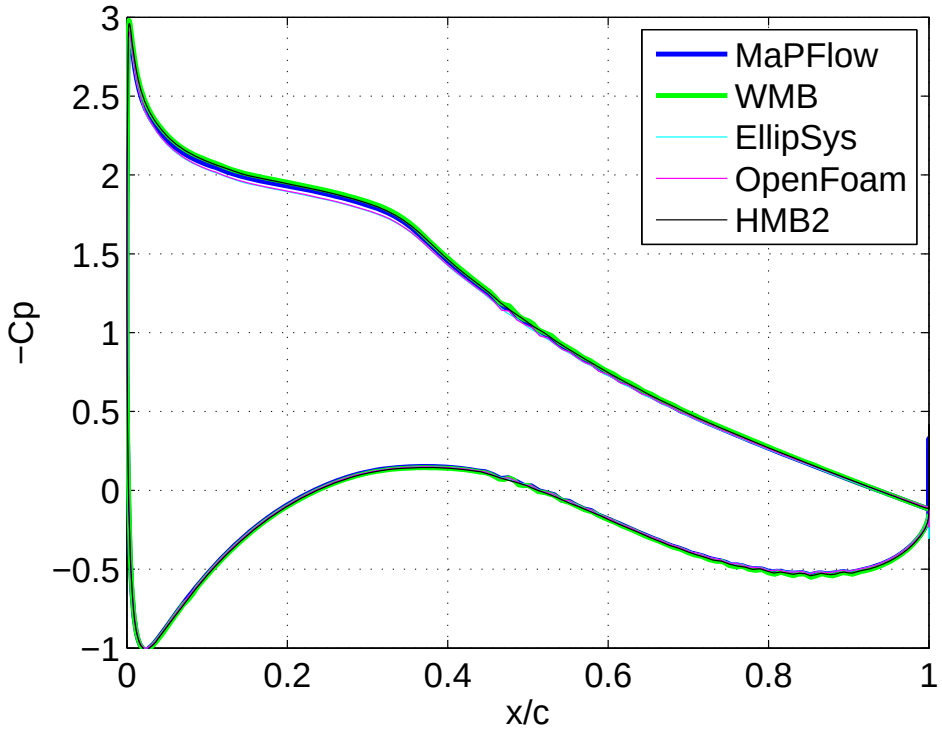

Figure 5: Pressure distribution for AoA 8, fully turbulent and Re=20×10^6

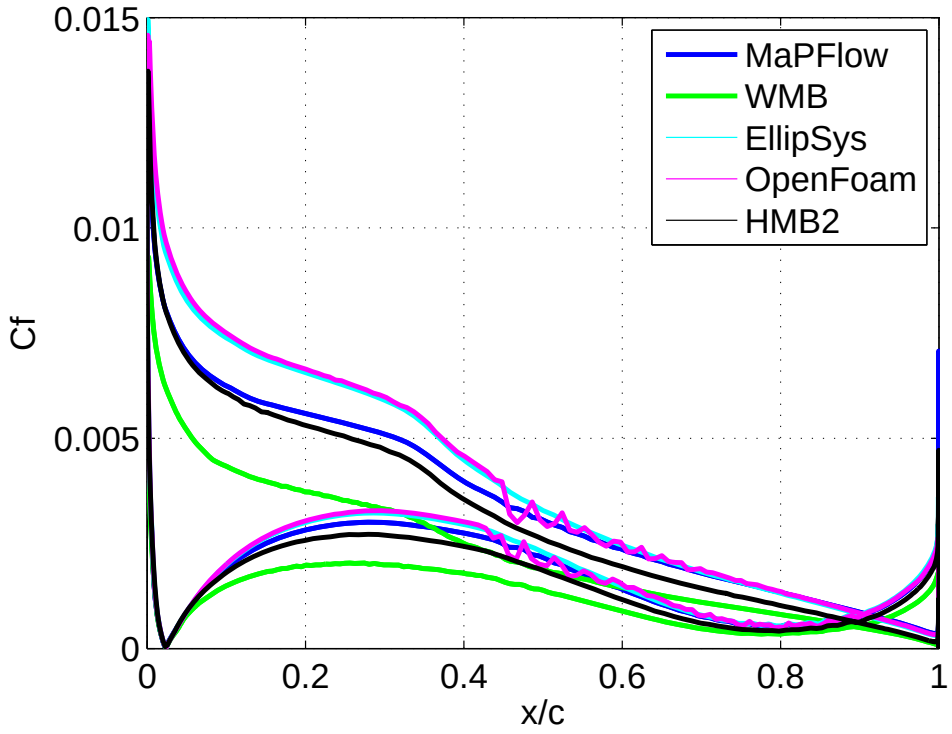

Figure 6: Skin friction distribution for AoA 8, fully turbulent and Re=20×10^6

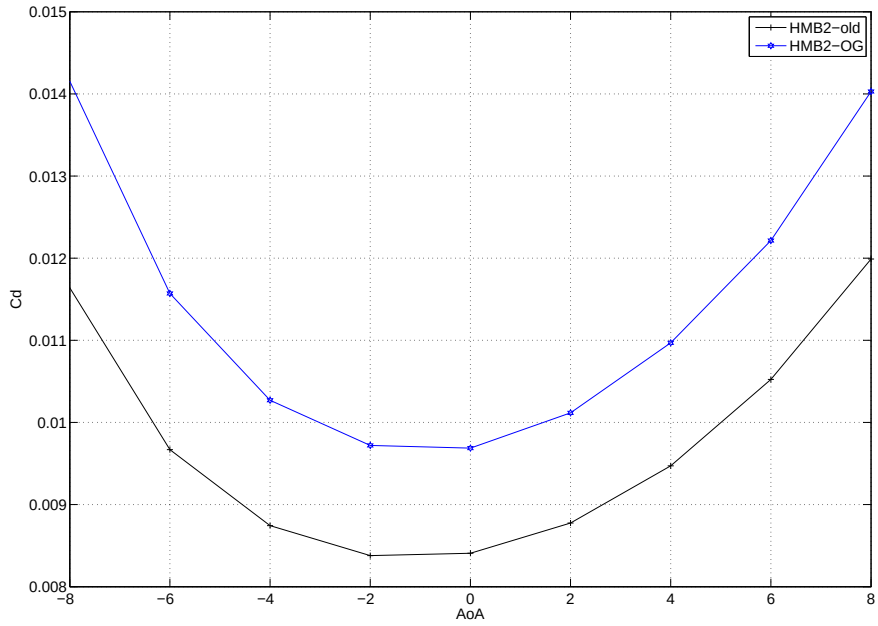

Figure 7: Computed drag using the HMB2 code on two different grids, fully turbulent and Re=20×10^6

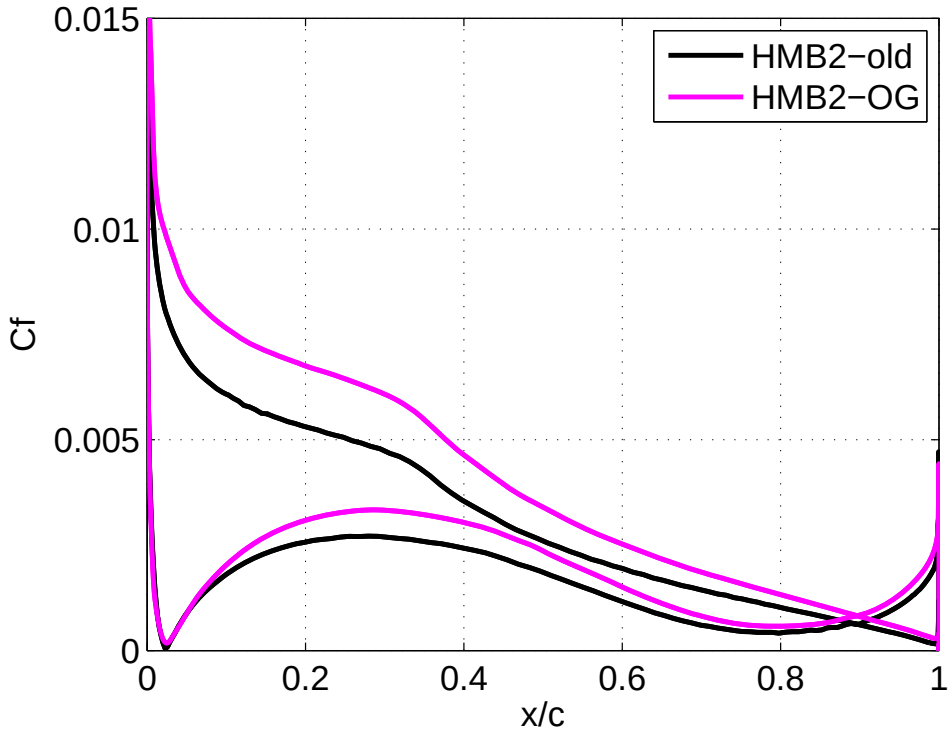

Figure 8: Skin friction distribution for AoA 8, fully turbulent and Re=20×10^6

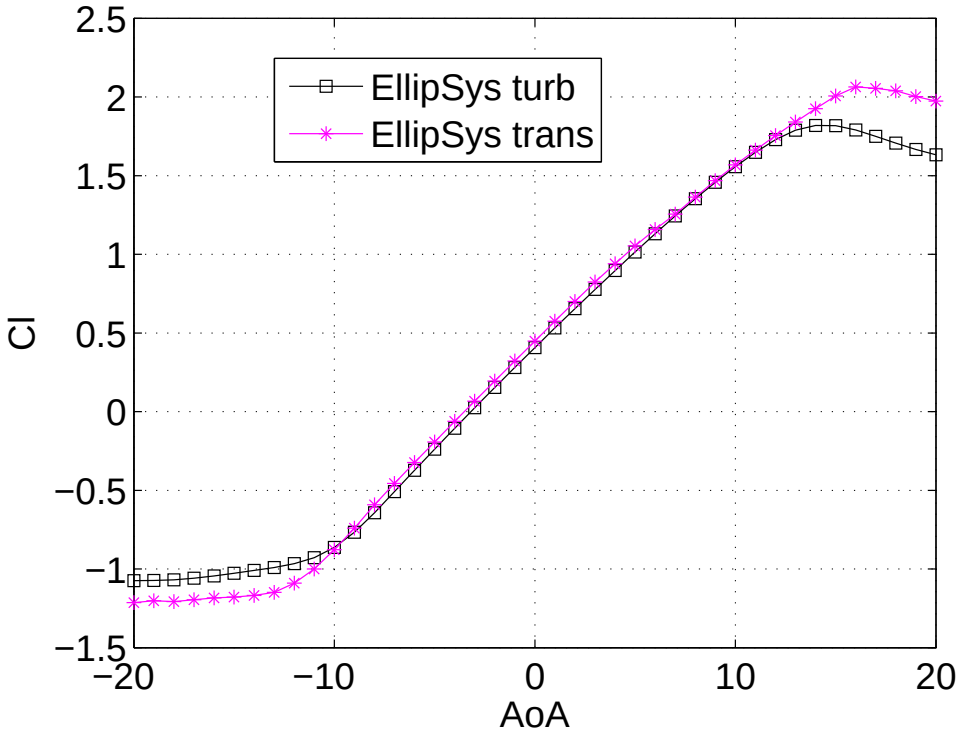

Figure 9: Lift vs AoA transitional and fully turbulent and Re=20×10^6

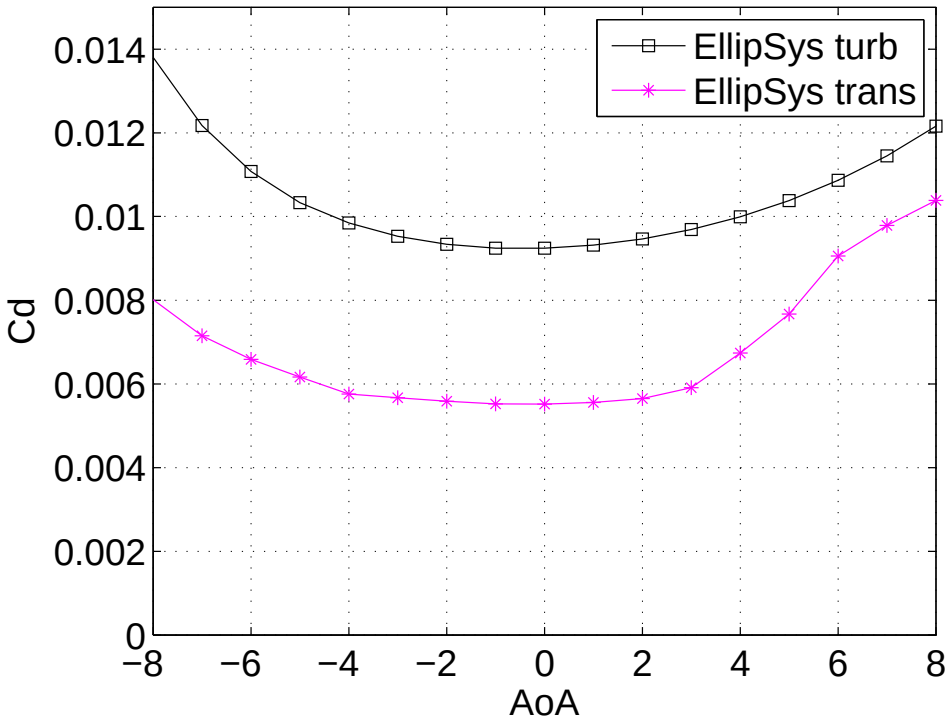

Figure 10: Drag vs AoA transitional and fully turbulent and Re=20×10^6

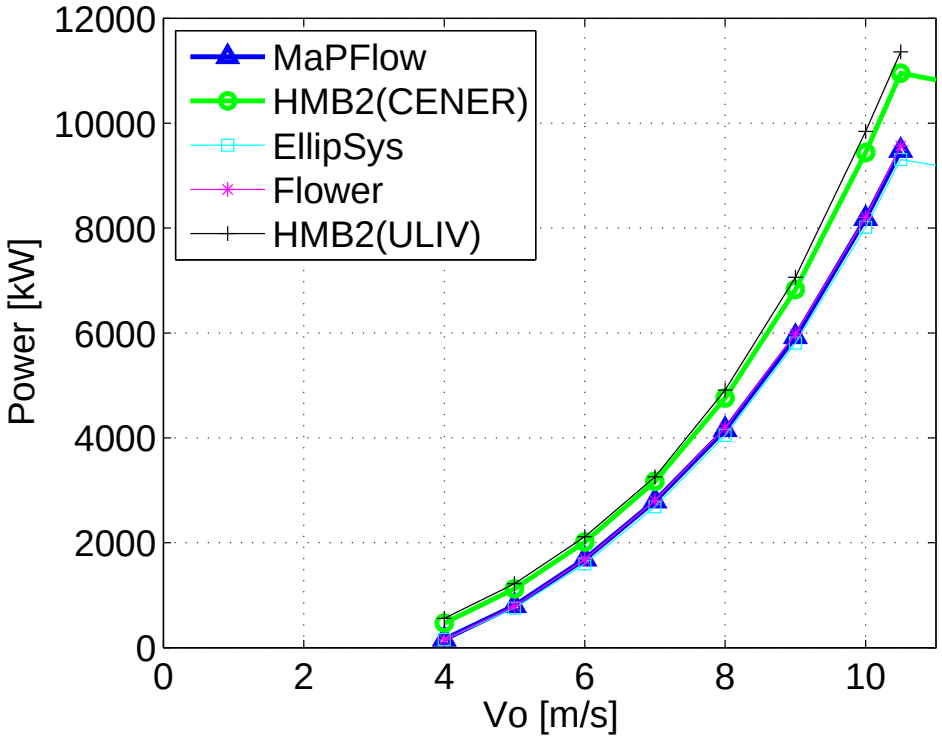

Figure 11: Computed powercurve for the AVATAR rotor assuming fully turbulent flow

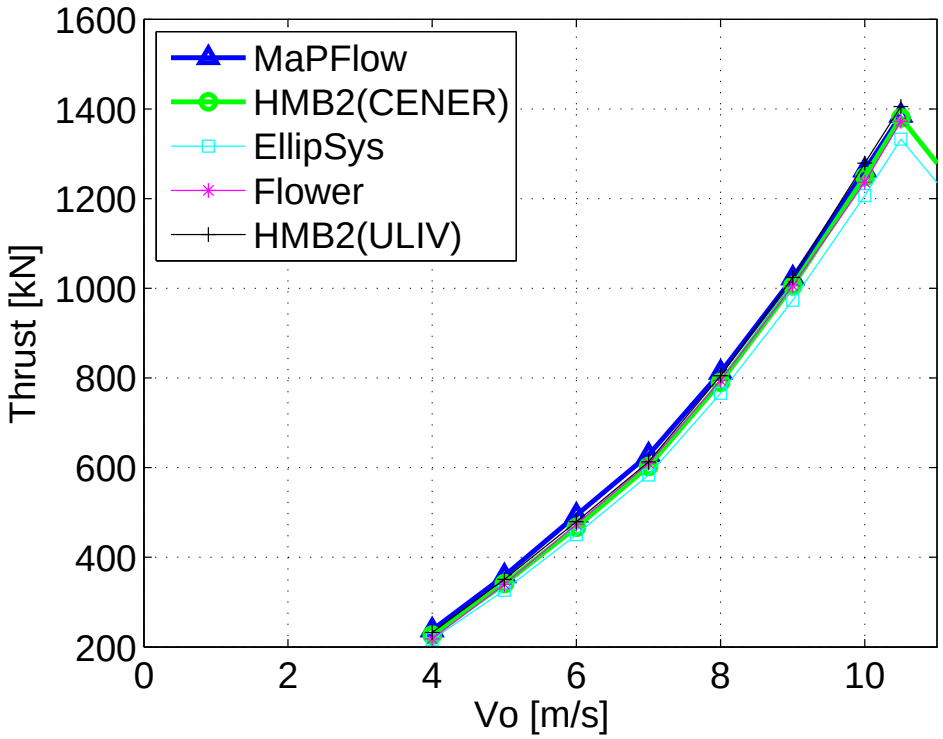

Figure 12: Computed thrust as function of wind speed for the AVATAR rotor assuming fully turbulent flow

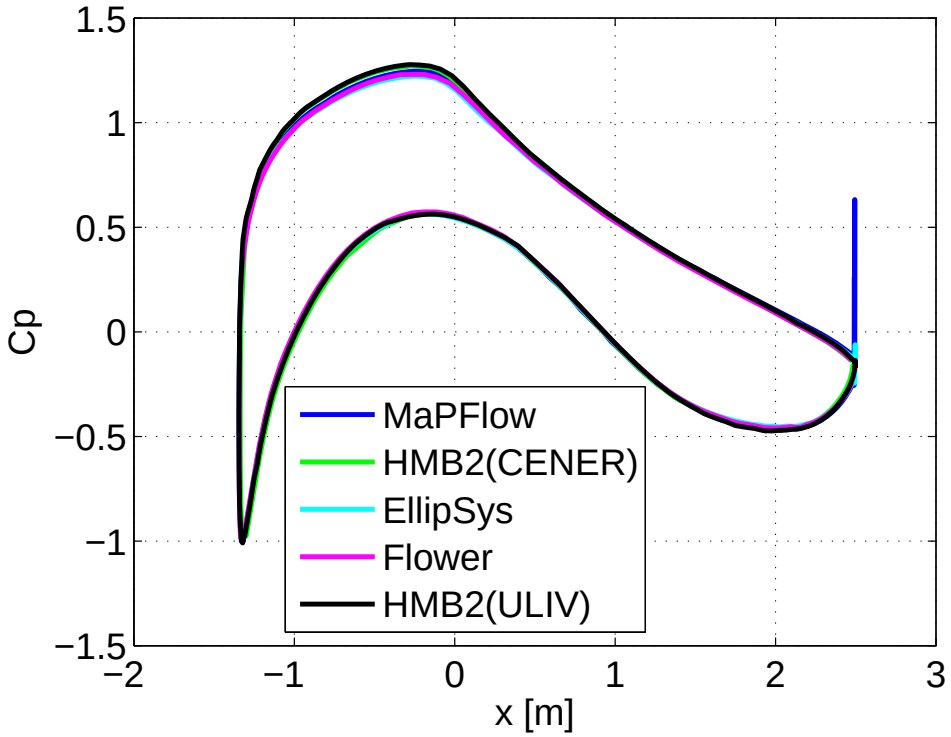

Figure 13: Chordwise pressure distribution at r=70 m, V_o=9 m/s for the AVATAR rotor assuming fully turbulent flow

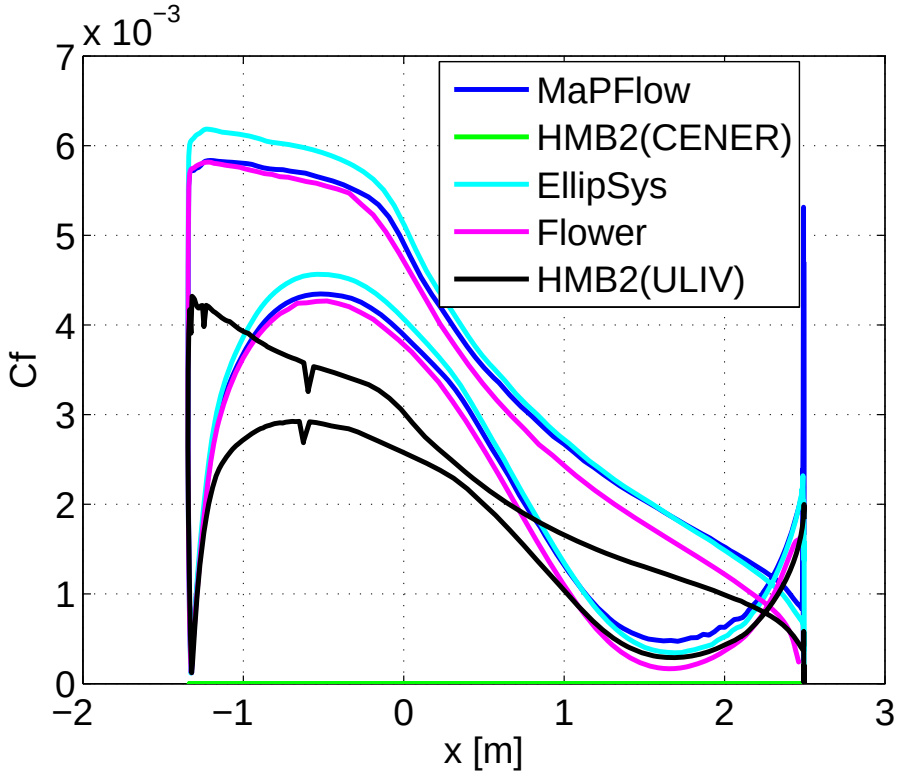

Figure 14: Chordwise skin friction distribution at r=70 m, V_o=9 m/s for the AVATAR rotor assuming fully turbulent flow

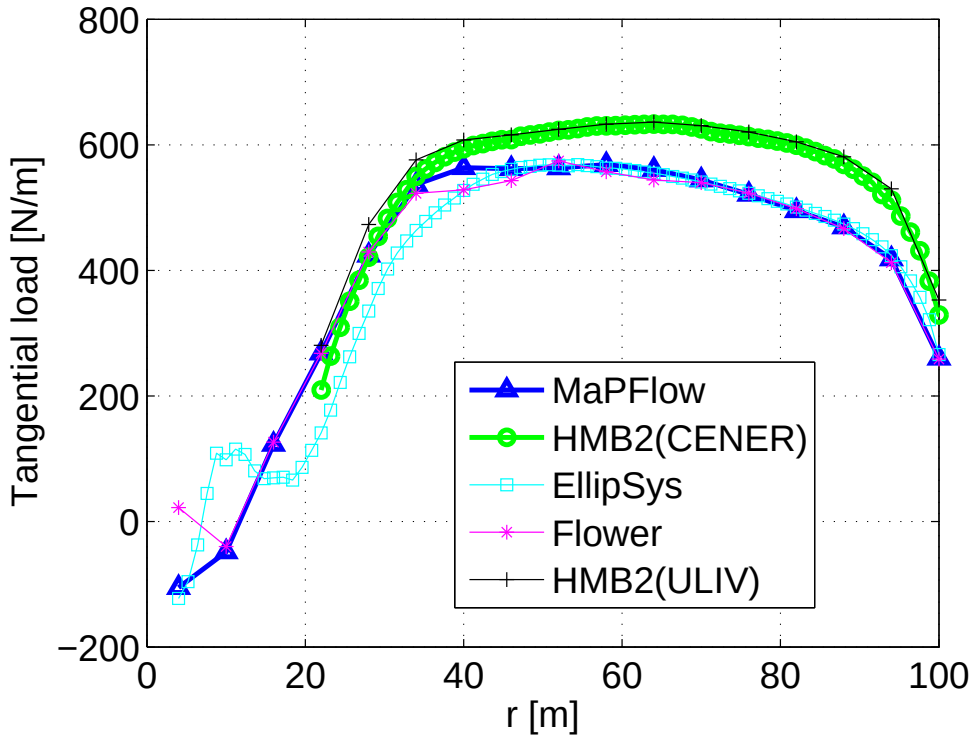

Figure 15: Tangential load distribution for the AVATAR rotor assuming fully turbulent flow at V_o=9 m/s

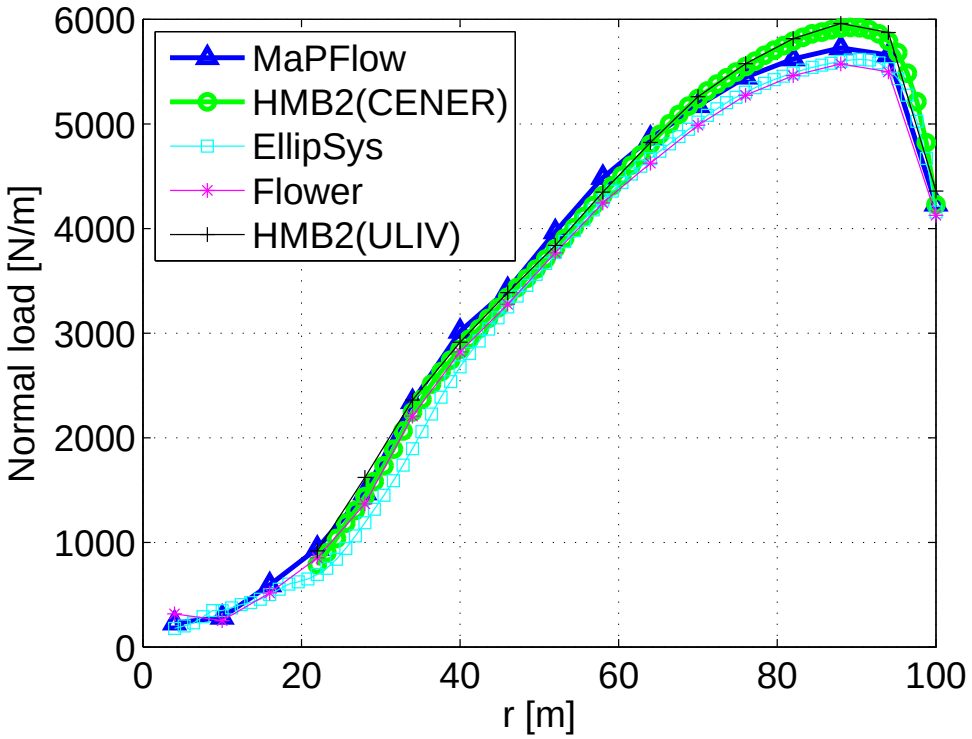

Figure 16: Normal load distribution for the AVATAR rotor assuming fully turbulent flow at at V_o=9 m/s

References

[1] Sorensen N.N., Zahle F., Michelsen J.A. Prediction of airfoil performance at high Reynolds numbers EFMC 2014

[2] Beatrice M. et al. 2-D Airfoil polars for the AVATAR rotor WP2 Deliverable 2.1

[3] N. N. Sørensen et al. 2D Airfoil Polars for the 24% Airfoil Section for the AVATAR Rotor WP2 Supplement to Delivery 2.1

[4] N. N. Sørensen et al. Power Curve Predictions WP2 Delivery 2.3